Supporting Information for

Regulation of the severity of neuroinflammation and demyelination by TLR-ASK1-p38 pathway

Xiaoli Guo, Chikako Harada, Kazuhiko Namekata, Atsushi Matsuzawa, Monsterrat Camps, Hong Ji, Dominique Swinnen, Catherine Jorand-Lebrun, Mathilde Muzerelle, Pierre-Alain Vitte, Thomas Rückle, Atsuko Kimura, Kuniko Kohyama, Yoh Matsumoto, Hidenori Ichijo, Takayuki Harada

Correspondence:

Takayuki Harada, M.D. Ph.D.

Department of Molecular Neurobiology

Tokyo Metropolitan Institute for Neuroscience

Tokyo Metropolitan Organization for Medical Research

2-6 Musashidai, Fuchu, Tokyo 183-8526, Japan.

Tel: +81-42-325-3881; Fax: +81-42-321-8678; E-mail: harada-tk@igakuken.or.jp

This PDF File Includes:

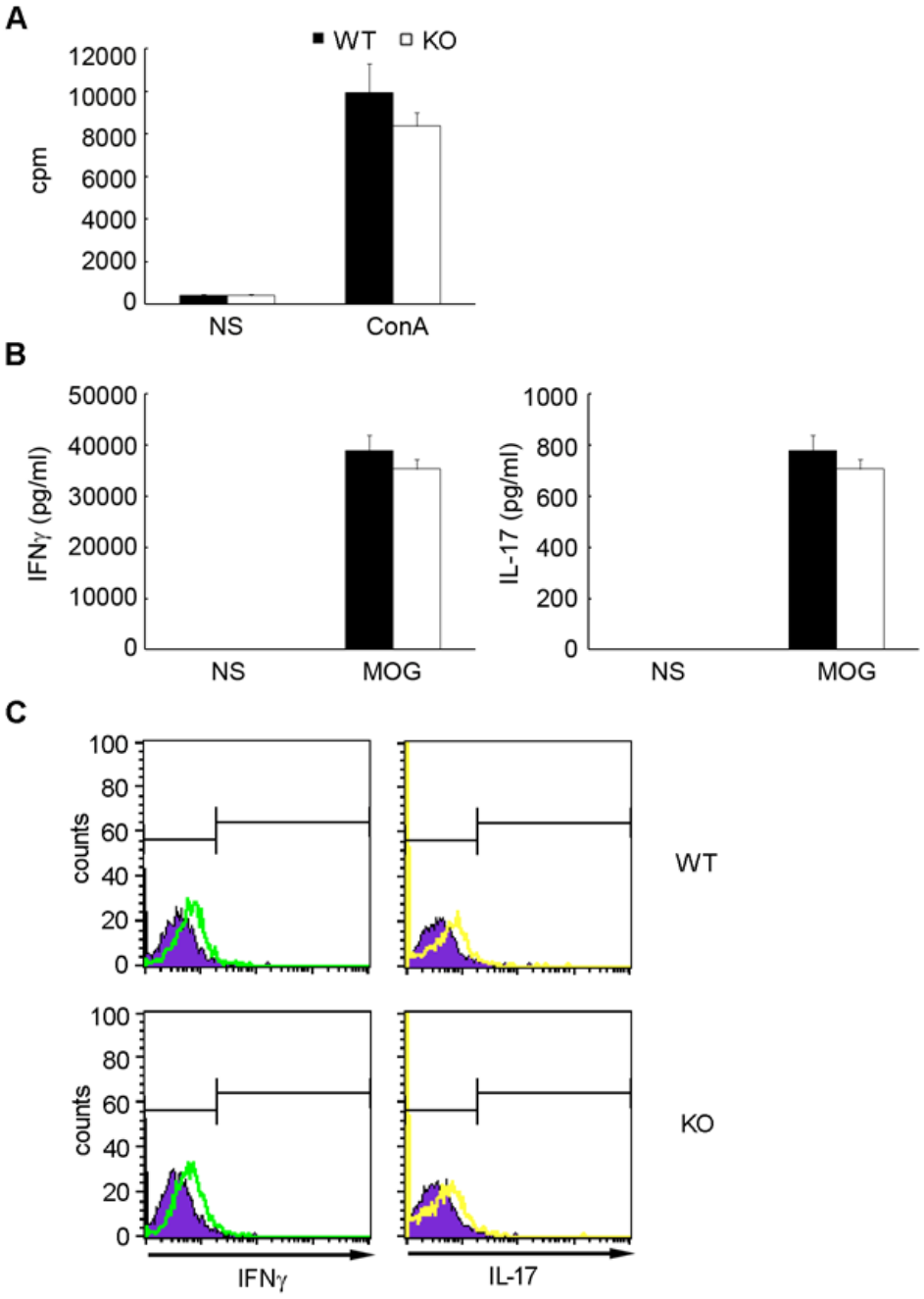

D

	IFNγ⁺	IL-17⁺
WT	1.41± 0.13	1.91± 0.1
KO	1.10± 0.25	1.33± 0.25
P	0.31	0.11

Figure S1. ASK1 deficiency had no effect on T cell response. (**A**) Proliferative responses of T cells isolated from WT and ASK1$^{-/-}$ (KO) mice (n = 4). Freshly isolated T cells were stimulated with or without ConA (10 μg/ml) for 3 days, with the last 18 h in the presence of 0.5 mCi [^{3}H]thymidine. (**B**) Cytokine releases from T cells stimulated by MOG (25 μg/ml) were measured by ELISA (n = 4). (**C**) Flow cytometric analysis of intracellular cytokine profiles in the spinal cords of EAE mice. Spinal cord-infiltrating leukocytes were purified from EAE mice at day 14 after MOG immunization and were analyzed for intracellular expression of the indicated markers by flow cytometry. Comparable percentages of IFNγ^{+} and IL-17^{+} cells infiltrate the CNS in ASK1$^{-/-}$ and WT EAE mice. Representative figures are shown. Purple area corresponds to unstained cells, while green and yellow indicate stained cells. (**D**) Percentages of IFNγ^{+} and IL-17^{+} cells. Results from 4 animals per genotype are presented as means ± SEM.

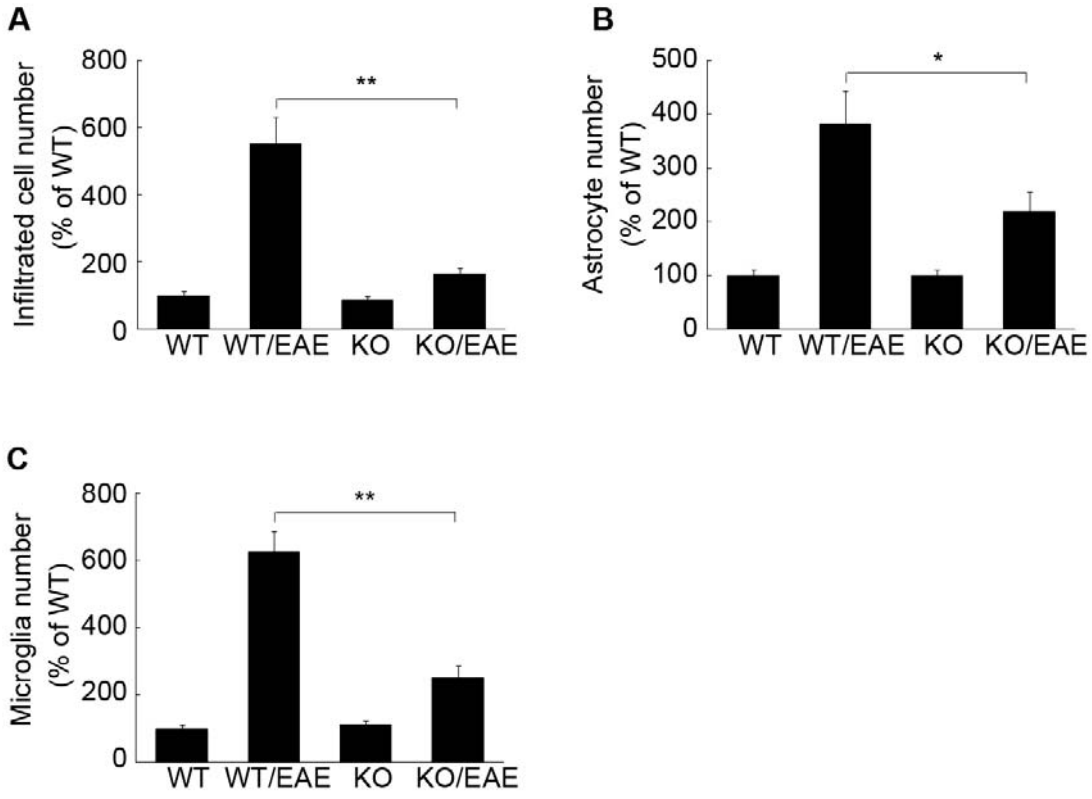

Figure S2. ASK1 deficiency attenuates EAE-induced CNS inflammation and glial activation in the spinal cord of ASK1$^{-/-}$ (KO) EAE mice. (**A**) Quantitative analysis of cell infiltrates in the white matter of the spinal cord. **(B, C)** Quantitative analysis of GFAP-positive **(B)** and iba1-positive **(C)** cells in the spinal cord. GFAP- and iba1-positive cells were counted per unit area (0.143 mm^2) in the middle region of the ventral horn. The number of cells was expressed as a percentage of the wild-type non-EAE (WT) mice. $^{**}P < 0.01$; $^{*}P < 0.05$.

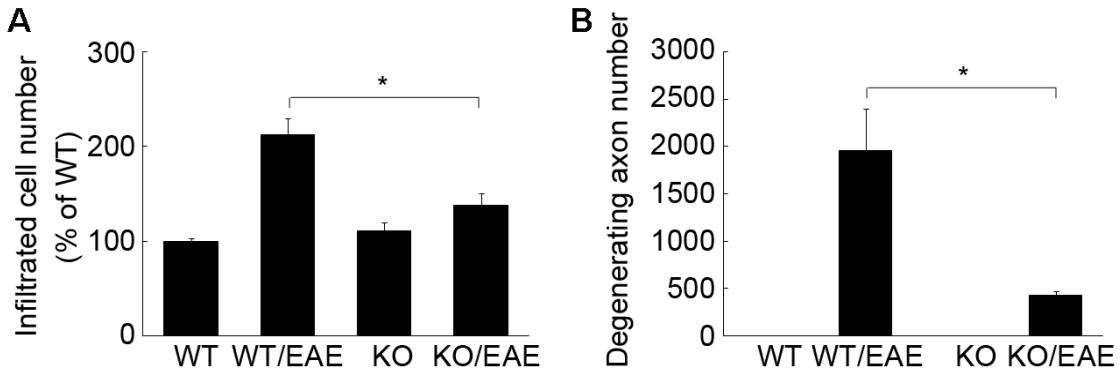

Figure S3. ASK1 deficiency attenuates EAE-induced cell infiltration and axon degeneration in the optic nerves of ASK1$^{-/-}$ (KO) EAE mice. **(A)** Quantitative analysis of cell infiltrates in the longitudinal section of the optic nerve. The number of cells was expressed as a percentage of the wild-type non-EAE (WT) mice. **(B)** Quantitative analysis of degenerating axons in the transverse section of the optic nerve. *$P < 0.05$.

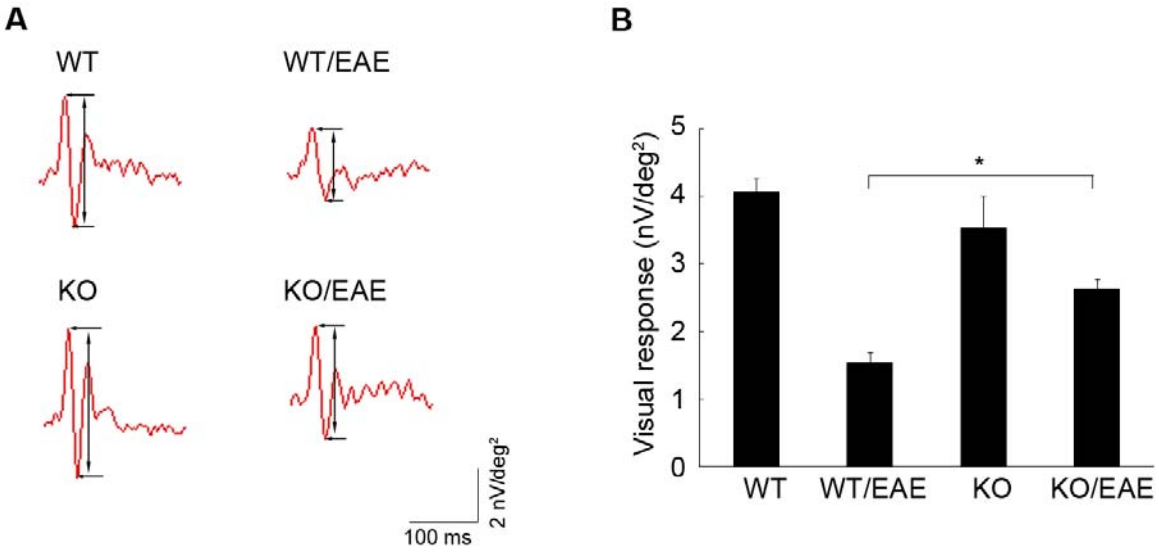

Figure S4. Improved visual function in ASK1$^{-/-}$ (KO) EAE mice. **(A)** Representative multifocal electroretinogram waveforms from each mouse group for the measurement of the response amplitude. **(B)** Quantitative analysis of the response amplitude. The response amplitudes for each stimulus element were added and the result was divided by the total area of the visual stimulus. *$P < 0.001$. Values are given in nV per square degree (nV/deg^2).

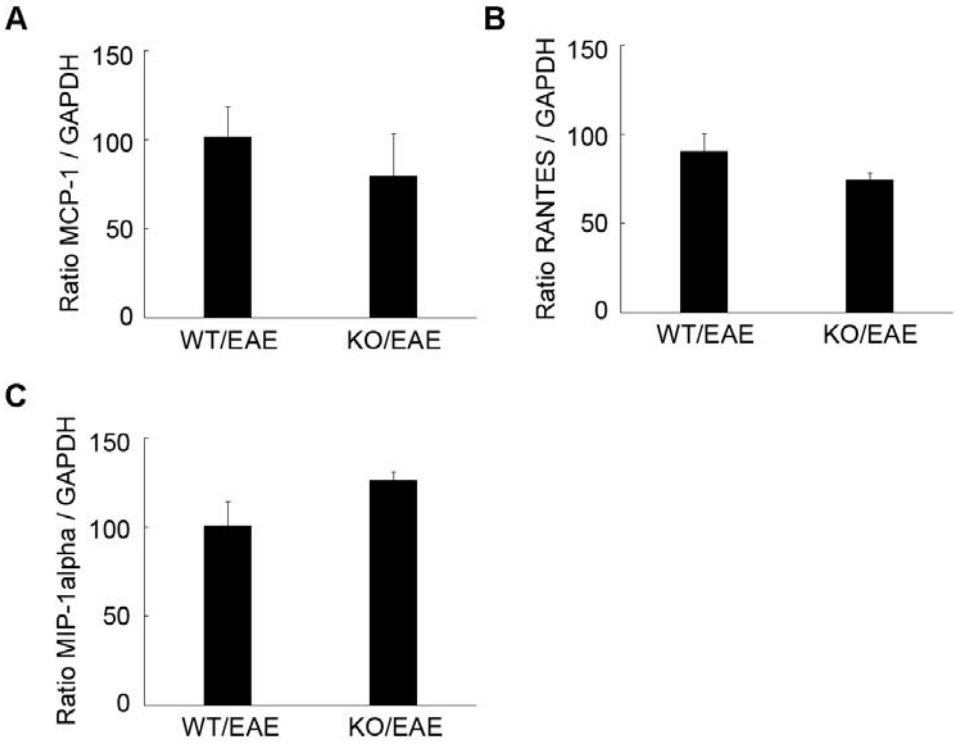

Figure S5. Chemokine production in the spinal cords of ASK1$^{-/-}$ EAE mice (n = 3) at d12 after MOG-immunization was comparable with WT EAE mice (n = 3). mRNA expression levels of MCP-1 **(A)**, RANTES **(B)** and MIP-1α **(C)** were determined using quantitative real-time PCR. GAPDH was used as an internal control.

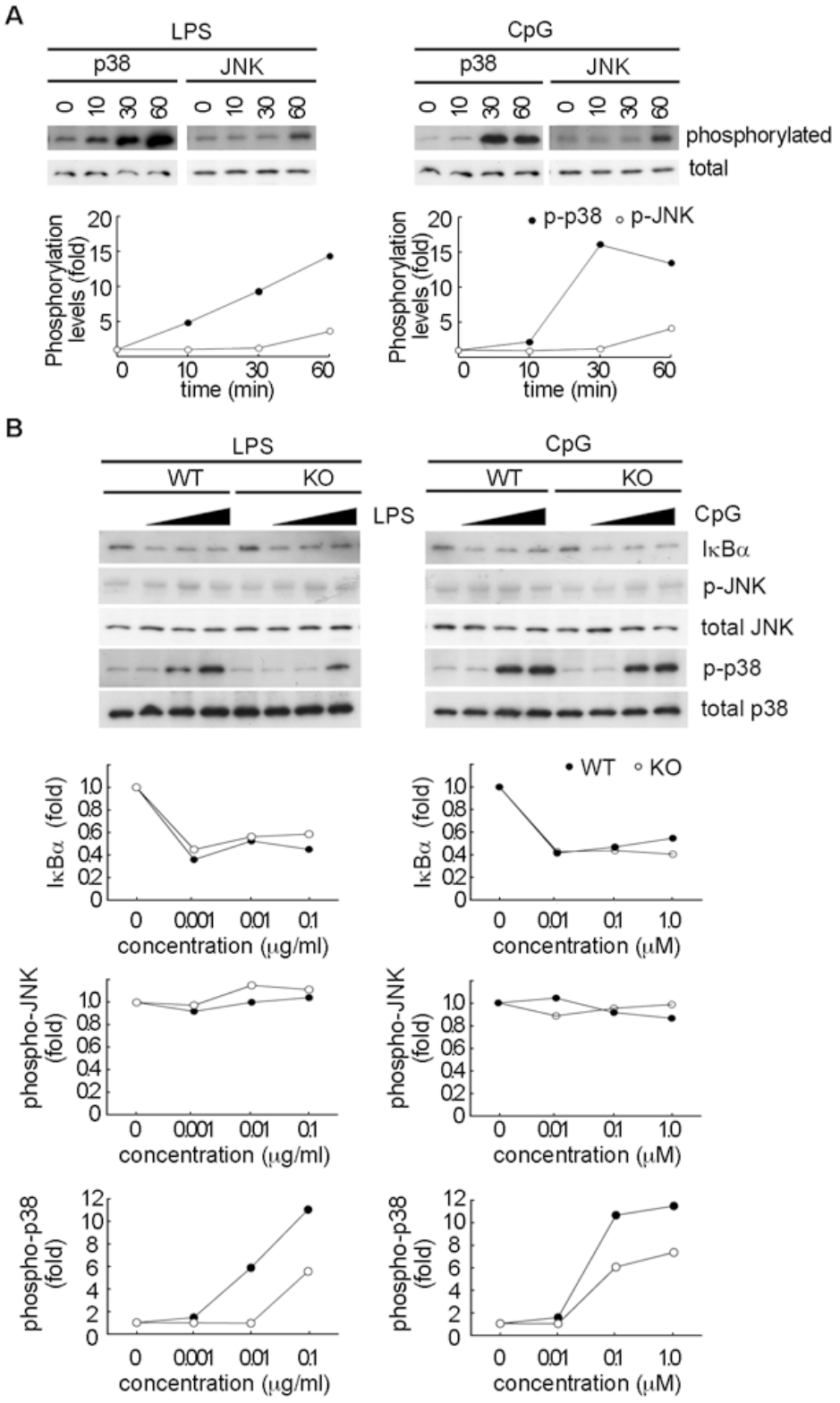
A
LPS
CpG
p38
JNK
0
10
30
60
phosphorylated
total
Phosphorylation levels (fold)
time (min)
p-p38
p-JNK
B
WT
KO
LPS
CpG
IκBα
p-JNK
total JNK
p-p38
total p38
IκBα (fold)
concentration (μg/ml)
concentration (μM)
phospho-JNK (fold)
phospho-p38 (fold)

Figure S6. ASK1 is required for TLR ligands-induced p38 activation in astrocytes. **(A)** Activation states of p38 and JNK in wild-type astrocytes stimulated with LPS (0.01 μg/ml) or unmethylated CpG DNA (0.1 μM) for the indicated time. Cell lysates were subjected to immunoblot analysis using antibodies to phosphorylated form of p38 (p-p38) or JNK (p-JNK). Membranes were reprobed with antibodies to total JNK and p38 as loading controls. p-p38 and p-JNK were quantified by densitometry analysis. **(B)** Analysis of NF-κB, JNK and p38 activation in astrocytes from wild-type (WT) or $ASK1^{-/-}$ (KO) mice treated with the indicated concentration of LPS or unmethylated CpG DNA for 30 min. The NF-κB activation was assessed by degradation of IκBα, an NF-κB inhibitor. Cell lysates were subjected to immunoblot analysis using antibodies against IκBα, p-JNK, total JNK, p-p38 and total p38.

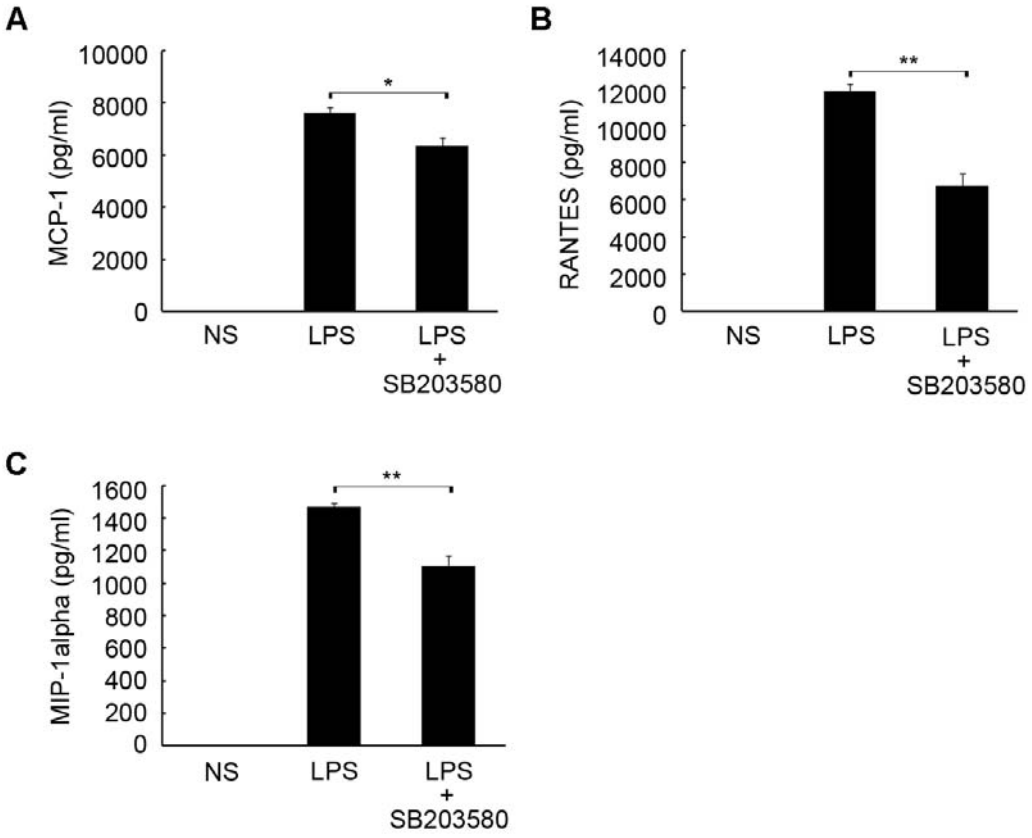

Figure S7. Chemokine production in astrocytes was inhibited by SB203580, a p38 inhibitor. Astrocytes isolated from WT mice were treated with SB203580 (2 μM) for 30 min prior to LPS stimulation (0.1 μg/ml) for 16 h. Concentrations of MCP-1 **(A)**, RANTES **(B)** and MIP-1α **(C)** in culture medium were measured by ELISA. $^{**}P < 0.01$; $^{*}P < 0.05$.

Table S1. Complete list of the selectivity of MSC2032964A against a panel of 210 kinases

	Kinase	% inhibition @ 10 μM
1	Abl(h)	-3
2	Abl(m)	16
3	Abl(T315I)(h)	5
4	ALK(h)	-23
5	ALK4(h)	-16
6	AMPK(r)	19
7	Arg(h)	-5
8	Arg(m)	-2
9	ARK5(h)	2
10	ASK1(h)	94
11	Aurora-A(h)	18
12	Axl(h)	0
13	Blk(m)	-7
14	Bmx(h)	-17
15	BRK(h)	2
16	BrSK1(h)	3
17	BrSK2(h)	-1
18	BTK(h)	-3
19	CaMKI(h)	0
20	CaMKII(r)	12
21	CaMKIV(h)	8
22	CDK1/cyclinB(h)	4
23	CDK2/cyclinA(h)	-2
24	CDK2/cyclinE(h)	-4
25	CDK3/cyclinE(h)	-9
26	CDK5/p25(h)	7
27	CDK5/p35(h)	-8
28	CDK6/cyclinD3(h)	-13
29	CDK7/cyclinH/MAT1(h)	-5
30	CDK9/cyclin T1(h)	1
31	CHK1(h)	-5
32	CHK2(h)	-1
33	CK1γ2(h)	70
34	CK1δ(h)	81
35	CK2(h)	-1
36	CK2α2(h)	16
37	cKit(D816V)(h)	0
38	cKit(h)	-15
39	CLK3(h)	-9
40	c-RAF(h)	-24
41	CSK(h)	-18
42	cSRC(h)	-2
43	DAPK1(h)	-2
44	DAPK2(h)	0
45	DDR2(h)	2
46	DMPK(h)	-12
47	DRAK1(h)	-2
48	DYRK2(h)	102
49	eEF-2K(h)	-9
50	EGFR(h)	6
51	EGFR(L858R)(h)	-13
52	EGFR(L861Q)(h)	-10

	Kinase	% inhibition @ 10 µM
53	EphA1(h)	-21
54	EphA2(h)	-4
55	EphA3(h)	-11
56	EphA4(h)	5
57	EphA5(h)	-12
58	EphA7(h)	-8
59	EphA8(h)	-14
60	EphB1(h)	6
61	EphB2(h)	-15
62	EphB3(h)	-1
63	EphB4(h)	-19
64	ErbB4(h)	2
65	Fer(h)	30
66	Fes(h)	12
67	FGFR1(h)	-23
68	FGFR2(h)	8
69	FGFR3(h)	-1
70	FGFR4(h)	1
71	Fgr(h)	-2
72	Flt1(h)	-4
73	Flt3(D835Y)(h)	20
74	Flt3(h)	19
75	Flt4(h)	22
76	Fms(h)	42
77	Fyn(h)	0
78	GCK(h)	11

	Kinase	% inhibition @ 10 µM
79	GSK3α(h)	34
80	GSK3β(h)	5
81	Haspin(h)	69
82	Hck(h)	13
83	HIPK1(h)	-1
84	HIPK2(h)	-8
85	HIPK3(h)	4
86	IGF-1R(h)	4
87	IKKα(h)	7
88	IKKβ(h)	-4
89	IR(h)	0
90	IRAK1(h)	-15
91	IRAK4(h)	-10
92	IRR(h)	2
93	Itk(h)	-9
94	JAK2(h)	-3
95	JAK3(h)	-8
96	JNK1α1(h)	-5
97	JNK2α2(h)	-7
98	JNK3(h)	71
99	KDR(h)	3
100	Lck(h)	1
101	LIMK1(h)	-32
102	LKB1(h)	8
103	LOK(h)	76
104	Lyn(h)	4

	Kinase	% inhibition @ 10 µM
105	Lyn(m)	-2
106	MAPK1(h)	5
107	MAPK2(h)	-2
108	MAPK2(m)	-11
109	MAPKAP-K2(h)	-9
110	MAPKAP-K3(h)	-1
111	MARK1(h)	-11
112	MEK1(h)	-5
113	MELK(h)	-20
114	Met(h)	-5
115	MINK(h)	-16
116	MKK4(m)	1
117	MKK6(h)	-10
118	MKK7β(h)	-6
119	MLCK(h)	-2
120	MLK1(h)	37
121	Mnk2(h)	90
122	MRCKα(h)	1
123	MRCKβ(h)	-4
124	MSK1(h)	-8
125	MSK2(h)	15
126	MSSK1(h)	-2
127	MST1(h)	0
128	MST2(h)	-10
129	MST3(h)	-8
130	MuSK(h)	-4

	Kinase	% inhibition @ 10 µM
131	NEK11(h)	-2
132	NEK2(h)	10
133	NEK3(h)	-6
134	NEK6(h)	-1
135	NEK7(h)	25
136	NLK(h)	-10
137	p70S6K(h)	-2
138	PAK2(h)	2
139	PAK3(h)	35
140	PAK4(h)	-5
141	PAK5(h)	-5
142	PAK6(h)	-17
143	PAR-1Bα(h)	1
144	PASK(h)	-6
145	PDGFRα(h)	-4
146	PDGFRβ(h)	-19
147	PDK1(h)	-8
148	Pim-1(h)	72
149	Pim-2(h)	5
150	PKA(h)	-15
151	PKBα(h)	4
152	PKBβ(h)	-7
153	PKBγ(h)	4
154	PKCμ(h)	7
155	PKCα(h)	16
156	PKCβI(h)	3

	Kinase	% inhibition @ 10 µM
157	PKCβII(h)	4
158	PKCγ(h)	3
159	PKCδ(h)	5
160	PKCε(h)	11
161	PKCζ(h)	-3
162	PKCη(h)	-1
163	PKCθ(h)	-4
164	PKCι(h)	65
165	PKD2(h)	14
166	PKG1α(h)	6
167	PKG1β(h)	-1
168	Plk3(h)	-11
169	PRAK(h)	40
170	PRK2(h)	-14
171	PrKX(h)	-4
172	PTK5(h)	6
173	Ret(h)	22
174	RIPK2(h)	-8
175	ROCK-I(h)	11
176	ROCK-II(h)	-5
177	ROCK-II(r)	-2
178	Ron(h)	-8
179	Ros(h)	-3
180	Rse(h)	5
181	Rsk1(h)	56
182	Rsk1(r)	53

	Kinase	% inhibition @ 10 µM
183	Rsk2(h)	64
184	Rsk3(h)	68
185	SAPK2a(h)	1
186	SAPK2a(T106M)(h)	-4
187	SAPK2b(h)	5
188	SAPK3(h)	-6
189	SAPK4(h)	-18
190	SGK(h)	0
191	SGK2(h)	1
192	SGK3(h)	4
193	SIK(h)	6
194	Snk(h)	-5
195	SRPK1(h)	3
196	SRPK2(h)	3
197	STK33(h)	-8
198	Syk(h)	4
199	TAK1(h)	42
200	TBK1(h)	1
201	Tie2(h)	3
202	TrkA(h)	86
203	TrkB(h)	-13
204	TSSK1(h)	11
205	TSSK2(h)	-11
206	WNK2(h)	84
207	WNK3(h)	96
208	Yes(h)	-2

	Kinase	% inhibition @ 10 μM
209	ZAP-70(h)	2
210	ZIPK(h)	1

Table S2. In vivo pharmacokinetics study of MSC2032964A in rats

Species/strain/sex:	Rat, Sprague Dawley Crl:CD (SD), male			
Age (in weeks)	8			
Administration routes	intravenous (iv) and oral (po) gavage			
Total number of animals	12; 9 (iv) and 3 (po)			
Administration volume	iv: 5 mL/kg os: 5 mL/kg			
Vehicle	iv: PEG400/saline (1:1 v/v) po: 0.5% Carboxymethylcellulose containing 0.25% Tween 20 in water			
Duration of treatment:	single treatment			
Group number/administration route	1/iv	2/po	3/iv for brain exposure	
Dosage (mg/kg), *as parent*	0.6	5	0.6	
Vehicle abbreviation	PEG/NaCl	CMC/Tw	PEG/NaCl	
Number of tested animals	3	3	6	
Plasma sampling time (iv)	0.083, 0.25, 0.5, 1.5, 4, 6 h (from a tail or sublingual vein) and 24 h (at sacrifice) from 3 rats (collection of brains at 24 h)			
Plasma sampling time (po)	0.25, 0.5, 1.5, 4, 6 h (from tail or sublingual vein) and 24 h (at sacrifice) from 3 rats			
Plasma sampling time (iv for brain exposure)	0.25, 0.5, 1, 24 h (at sacrifice) from 2 rats/each sampling time			
Notes	No clinical abnormalities were seen in any animal either treated by oral or intravenous route. Blood sampling was difficult in all i.v. treated animals up to the 1.5 h sampling time.			

Table S3. MSC2032964A concentrations in plasma

Plasma concentrations (ng/mL) and bioavailability data					Individual values					
	IV-mean	**PO-mean**	**IV-stdev**	**PO-stdev**	**IV**	**IV**	**IV**	**PO**	**PO**	**PO**
Animal ID					**1**	**2**	**3**	**1**	**2**	**3**
Time (h)										
0	532.7	0.0	334.0	0.0	526.5	869.7	201.8	0	0	0
0.083	458.5	--	233.2	-	516.4	657.3	201.8	-	-	-
0.25	426.7	128.3	62.9	42.7	496.5	374.3	409.3	156.9	148.9	79.2
0.5	316.7	58.8	120.5	27.1	380.9	391.5	177.7	62.6	83.9	30.1
1.5	113.7	291.2	70.4	82.7	193.6	86.7	60.7	375.6	287.7	210.3
4	17.7	383.7	13.4	63.2	31.9	16.0	5.2	420.5	419.8	310.7
6	0.6	262.6	0.5	35.1	1.1	0.6	BQL	239.5	303.0	245.4
24	BQL	0.5	-	0.8	BQL	BQL	BQL	BQL	1.4	BQL
AUC_Z (h*ng/mL)	603.9	2617.7			839.5	629.3	342.8	1921.3	4580.7	1351.1
AUC_∞ (h*ng/mL)	606.1	4160.7			840.5	629.8	348.0	4467.4	4585.7	3429.0
Fz	-	0.52			-	-	-	-	-	-
F_∞	-	0.82			-	-	-	-	-	-
Cmax (ng/mL)	527.7	383.7			516.4	657.3	409.3	420.5	419.8	310.7
T_{max} (h)	0.139	4.0			0.083	0.083	0.25	4	4	4
$T_{1/2}$ (h)-estimate	0.646	5.2			0.61	0.64	0.69	7.37	2.40	5.87
$T_{1/2}$ range (h)	0.083-0.5	3.2-12			1.5-6	1.5-6	0.5-4	1.5-6	4-24	4-6
Cl (L/h/kg)	1.13	-			0.71	0.95	1.72	-	-	-
Vss (L/kg)	1.02	-			0.82	0.80	1.44	-	-	-
Vz (L/kg)	1.07	-			0.63	0.88	1.72	-	-	-

*BQL: Below the quantification limit: 0.5 ng/mL. Values in italics are calculated (C_0).

Table S4. Brain exposure of MSC2032964A (concentrations in ng/g)

Pooled samples (n = 2)	**Plasma**	**Brain**	**CSF**	**Spinal cord**	**Brain/Plasma**
Time (h)					
0.25	459.0	194.8	16.9	87.7	0.42
0.5	381.0	139.0	10.5	64.4	0.36
1	188.0	95.0	6.9	48.0	0.51
24	BQL	BQL	BQL	BQL	-

*BQL: Below the quantification limit: 0.5 ng/mL.

Table S5. Sequences of PCR primers used in this study

Primers	Nucleotide sequences (5'-3')
MCP-1	
Sense	5'- AACTGCATCTGCCCTAAGGT -3'
Antisense	5'- ACGGGTCAACTTCACATTCA -3'
RANTES	
Sense	5'- GCCCACGTCAAGGAGTATTT -3'
Antisense	5'- TGACAAACACGACTGCAAGA -3'
MIP-1α	
Sense	5'- AGATTCCACGCCAATTCATC -3'
Antisense	5'- CAGATCTGCCGGTTTCTCTT -3'
TLR3	
Sense	5'- GTGCATCGGATTCTTGGTTT -3'
Antisense	5'- TTCCCAGACCCAGTCTCTGT -3'
TLR4	
Sense	5'- GCCGGAAGGTTATTGTGGTA -3'
Antisense	5'- TGCCATGTTTGAGCAATCTC -3'
TLR9	
Sense	5'- CAGCCCTGACTAGGGACAAC -3'
Antisense	5'- CGGGAACCAGACATGAAGAT -3'
iNOS	
Sense	5'- ACTGTGTGCCTGGAGGTTCT -3'
Antisense	5'- GGCAGCCTCTTGTCTTTGAC -3'
GAPDH	
Sense	5'- TGCACCACCAACTGCTTAG -3'
Antisense	5'- GGATGCAGGGATGATGTTC -3'

Supporting Materials and Methods

Immunohistochemistry

On day 40 after immunization, wild-type (WT) non-EAE, WT EAE, ASK1$^{-/-}$ (KO) non-EAE, KO EAE mice were anesthetized with diethylether and perfused transcardially with saline, followed by 4% paraformaldehyde in 0.1 M phosphate buffer containing 0.5% picric acid. Optic nerves and lumbar spinal cords were removed, postfixed and processed for specific purposes respectively. Optic nerves were embedded in paraffin wax or Epon812 resin, sectioned and stained with luxol fast blue (LFB) followed by hematoxylin and eosin (H&E). Transversal semithin sections (500 nm) of the optic nerve were stained with toluidine blue. On the other hand, spinal cords were embedded in paraffin wax or optimal cutting temperature (OCT) compound (Tissue-Tek, Tokyo, Japan) and frozen on dry ice. Paraffin sections (7 μm) or cryostat sections (10 μm) were cut coronally and collected on MAS-coated slides (Matsunami, Osaka, Japan). For pathological study, sections were stained with LFB followed by H&E. Immunohistochemistry was performed as previously described (Harada *et al*, 2006). Briefly, the sections were blocked with phosphate-buffered saline (PBS; pH 7.4) containing 1% normal horse serum and 0.4% Triton-X 100 for 1 h at room temperature. They were incubated overnight at 4°C with the following primary antibodies: rabbit anti-iba1 (1.0 μg/ml) (Harada *et al*, 2002) and mouse anti-GFAP (50 μg/ml; Progen, Heidelberg, Germany), markers for microglia and astrocytes, respectively. For the double staining of TLRs with astrocytes or microglia cells, the sections were incubated with goat anti-TLR4 (2.0 μg/ml; Santa Cruz, CA) and mouse anti-GFAP (50

μg/ml; Progen) or rabbit anti-iba1 (1.0 μg/ml) (Harada *et al*, 2002), or mouse anti-TLR9 (1.0 μg/ml; Santa Cruz) and rabbit anti-GFAP (ab929, Abcam, Cambridge, United Kingdom) or rabbit anti-iba1 (1.0 μg/ml) (Harada *et al*, 2002). The sections were then incubated with Cy-2-conjugated donkey anti-mouse IgG (Jackson ImmunoResearch, West Grove, PA), Cy-2-conjugated donkey anti-rabbit IgG (Jackson ImmunoResearch), Cy-3-conjugated donkey anti-goat IgG or DAKO EnVision (DAKO, Glostrup, Denmark) and DAB substrate kit (DAKO).

Microscopy and quantification

Stained sections were examined with a microscope (BX51; Olympus, Tokyo, Japan) equipped with Plan Fluor objectives connected to a DP70 camera (Olympus). To quantify cell infiltrates in the optic nerve, infiltrated cell numbers were counted in selected areas in the longitudinal optic nerve and the cell densities were calculated. The degenerating axons across the whole transverse section of the optic nerve were counted and the density was calculated. To quantify single immunostaining results, sections from the spinal cord were examined and digital images from a same area (0.143 mm^2) of the middle region of the ventral horn were captured. Subsequently, iba1-, GFAP-positive cells in each group were counted from the images. The counting results for each group were averaged and expressed as mean percentage changes compared with age matched WT non-EAE group. To quantify immunostaining results of TLRs in astrocytes or microglia cells, digital images from the ventral region of the spinal cord were captured. Areas of the double stained regions were

measured with NIH Image (ImageJ 1.38) and normalized with the results measured from WT non-EAE mice.

Leukocyte isolation and flow cytometry

Isolation of spinal cord-infiltrating leukocytes was performed as follows. Spinal cords were removed from mice and homogenized. After centrifugation of spinal cord homogenates, infiltrating leukocytes were separated on a discontinuous percoll gradient (GE Healthcare, Buckinghamshire, UK). For intracellular cytokine profiles, cells were fixed, permeabilized and stained with a mouse Th1/Th2/Th17 phenotyping cocktail (BD Biosciences, San Jose, CA). The cells were analyzed using the BD FACSCalibur flow cytometer with BD CellQuest Pro software (BD Biosciences).

In vivo pharmacokinetics study in rats

In vivo pharmacokinetics study of MSC2032964A was performed in 8 week-old male Sprague-Dawley rats. Details on the compound administration, plasma sampling etc were listed in Table S2. Rats were dosed intravenously (i.v.) or by oral gavage. MSC2032964A was prepared in solution at 0.6 mg/kg for i.v. route (PEG 400 / Saline 1:1 v/v) and in suspension at 5 mg/kg (0.5% carboxymethylcellulose suspension, containing 0.25% Tween 20 in water) for oral gavage. Pharmacokinetics profile was obtained from 3 animals per dosing route. The volume of administration was 2 mL/kg for i.v. dosing and 5 mL/kg for

oral gavage. Blood samples (100 μL) were collected at 0.083 (5 min), 0.25, 0.5, 1, 4, 7 and 24 h post-dose for i.v. dosing, and at 0.5, 1, 4, 7 and 24 h for oral dosing, into heparin-Li+ containing tubes. Serial blood samples were collected from the tail or sublingual veins up to 24 hrs after dosing under light isoflurane anesthesia, and stored on ice until centrifugation. Plasma samples were stored frozen until analysis (-20 °C to -70 °C). For bioanalysis, samples were processed by protein precipitation (acetonitrile, formic acid 0.1%, addition of 3 volumes) after addition of one internal standard and analyzed using a sensitive and selective LC/MS/MS method. An aliquot of the resulting supernatant was subjected to LC/MS/MS analysis using a reverse phase column [Waters Xterra, C8, (3.5 μm particle size, 2.1 x 50 mm)] and a short gradient (1 min) from (Solvent A) 85% water, 15% acetonitrile and 0.1% formic acid to (Solvent B) 90% acetonitrile, 10% water and 0.1% formic acid followed by isocratic conditions of Solvent B for 3.5 min at 0.4 mL/min. Column effluent was monitored using a Sciex API 4000 triple quadrupole mass spectrometer with a Turbo V electrospray ion source. Unknown concentrations of test compounds were determined using a calibration curve ranging from 1 to 3000 ng/mL. Pharmacokinetic parameters were determined using non-compartmental analysis.

Microsome stability assay

Rat and human microsomes were used to screen the metabolic instability resulting from phase I oxidation. Microsomes (final concentration 0.5 mg/mL), 0.1M phosphate buffer pH 7.4 and test compound (final concentration 3 μM, 1% DMSO) were added to the assay plate

and pre-incubated at 37°C. NADPH solution (final incubation concentration of 1 mM) was added to initiate the reaction. The reaction is terminated by the addition of 100 µL of cold acetonitrile at the appropriate time points (time 0, 15, 30 and 45 min). The samples are centrifuged at 5000 rpm for 5 min at 4 °C to precipitate the protein. Samples were analyzed by LC/MS-MS. The percentage of compound disappearance, the *in vitro* intrinsic clearance was calculated.

Caco-2 permeability

Caco-2 cells were obtained from American Type culture collection (Rockville, MD). The cells were seeded onto 24-well polycarbonate filter membrane (Transwell inserts, surface area: 0.33 cm^2, Corning, Tokyo, Japan) at a cell density of $1x10^5$ cell/cm^2 and grown in Dulbecco's modified Eagle's medium supplemented with 10% fetal bovine serum, 1% nonessential amino acids, 1% L-glutamine. Permeability studies were performed with the monolayers cultured for 21 days. Prior to all experiments, the cell monolayer integrity was evaluated by trans epithelial electrical resistance (TEER), values greater than 800 ohm·cm^2 were used. The permeability studies were initiated by adding an appropriate volume of Hank's balanced salt solution buffer containing 10 µM test compound to either the apical (for apical to basolateral transport; A to B) or basolateral (for basolateral to apical transport; B to A) side of the monolayer. The monolayers were then placed in an incubator at 37 °C. At the end of the incubation time (2 h) samples were taken from both the apical and basolateral compartments. The concentrations of test compound were analyzed by

LC/MS-MS. Permeability coefficient (Papp) was calculated according to the following equation: Papp= $dA/(dt \cdot S \cdot C_0)$, where dA/dt is the flux of the test compound across the monolayer (nmol/s); S is the surface area of the cell monolayer (cm^2); and C_0 is the initial concentration (μM) in the donor compartment.

Supporting References

Harada T, Harada C, Kohsaka S, Wada E, Yoshida K, Ohno S, Mamada H, Tanaka K, Parada LF, Wada K (2002) Microglia-Müller glia cell interactions control neurotrophic factor production during light-induced retinal degeneration. J Neurosci 22: 9228-9236

Harada C, Nakamura K, Namekata K, Okumura A, Mitamura Y, Iizuka Y, Kashiwagi K, Yoshida K, Ohno S, Matsuzawa A *et al* (2006) Role of apoptosis signal-regulating kinase 1 in stress-induced neural cell apoptosis *in vivo*. Am J Pathol 168: 261-269